16th Australasian Fluid Mechanics Conference
Crown Plaza, Gold Coast, Australia
2-7 December 2007

Effect of Initial Conditions on the Scalar Decay in Grid Turbulence at Low R_λ

A. Benaissa[1], L. Djenidi[2], R. A. Antonia[2], R. Parker[2]

[1]Department of Mechanical Engineering, Royal Military College of Canada, Kingston Ontario, Canada
[2] Disciplines of Mechanical Engineering, University of Newcastle, NSW, 2308 Australia

Abstract

Decaying grid turbulence is considered at low Reynolds number (R_λ ~ 50) for different initial conditions. Three different grid geometries are used. Heat is injected via a mandoline at a distance of 1.5 M from the grid. The amount of heating is such that temperature may be treated as a passive scalar. A small contraction (1.36:1) is added at a distance of 11M downstream of the grid. The power-law exponents for the scalar variance are compared with those for the turbulent kinetic energy. These exponents depend on the grid geometry.

For the isotropic dissipation rate $\langle\chi\rangle_{iso}$, the power-law exponent agrees with that inferred from the temperature variance transport equation. Restricting the range of validity of the decay law affects the magnitudes of the origin and decay exponent. Second-order temperature structure functions collapse when the normalization is based on the local temperature variance and the Corrsin microscale but the asymptotic form of this collapse depends on the initial conditions.

Introduction

Grid turbulence has been extensively studied because it represents an approximation to homogenous isotropic turbulence. The similarity analysis of this flow has given a clear view of the concept of universal behaviour of turbulence. From the large amount of literature available on the subject (e.g. [1,2,3,4,5]) and in the recent work of Lavoie *et al*. [10], it has become clear that George's [7] ideas about the influence of initial conditions on similarity need to be carefully taken into account.

Lavoie *et al.* [8,9,10] clearly established that the decay law of mean turbulent energy depends on the organization of the flow downstream of the grid. The nature of this organization imposes a range of validity on the decay law which differs from grid to grid, at nominally the same R_λ.

Different grids were used to study decay laws of different dynamic properties (the mean turbulent energy, the mean turbulent energy dissipation rate and the entropy). A contraction was also used to improve isotropy (mainly at the large scales), as described in [6] and [15]. The contraction reduced the anisotropy of the large scales and yielded an improved approximation to HIT. It also lessened the importance of initial conditions on the scaling range and its exponent.

For the decay of the temperature variance, previous studies [1,3,17] have yielded different decay exponents, most likely reflecting differences in initial conditions, which have not always been adequately described. Zhou *et al.* [17] showed that the decay law exponent of $\langle\chi\rangle$ (the mean dissipation rate of $\langle\theta^2\rangle/2$) and $\langle\chi\rangle_{iso} = 3k\left\langle\left(\partial\theta/\partial x\right)^2\right\rangle$ are the same. $\langle\chi\rangle$ is given by:

$$\langle\chi\rangle = 2\kappa\int_0^\infty \mathsf{k}^2\phi(\mathsf{k})d\mathsf{k} \tag{1}$$

and the temperature variance $<\theta^2>$ is given by

$$\langle\theta^2\rangle = \int_0^\infty \phi(\mathsf{k})d\mathsf{k} \tag{2}$$

George [7] showed that the equation for scalar spectrum satisfied similarity (at all scales) with $\langle\theta^2\rangle$ as the relevant temperature scale and the Corrsin microscale scale $\lambda_\theta \sim (x)^{1/2}$ as the relevant length scale. The exponent n in the variance decay law depends on initial conditions.

Introducing the notion of effective origin for the decay, we can write:

$$\langle\theta^2\rangle = A_\theta(x/M - x_0/M)^n \tag{3}$$

and $$\lambda_\theta^2 = -\frac{6k(x-x_0)}{nU} \tag{4}$$

which leads to $$\lambda_\theta^2/M(x-x_0) = -\frac{6k}{nUM^2} = const \tag{5}$$

This latter relationship was used by Antonia *et al*. [3] to determine x_0 and n over a wide range of x/M, between 30 and 80.

In the present study, we analyse the effect of initial conditions on the decay of the temperature variance. Three different grids already used in Lavoie *et al.* are chosen [10] and only the Power Law Decay Range (PLDR), where the decay law is satisfied, is considered. Because only the test section with the secondary contraction is used, the following definition is adopted:

$x = tU_0$, where t is defined as in Comte-Bellot and Corrsin [6].

$$t = \int_0^x \frac{ds}{U(s)} \tag{6}$$

Structure functions are also calculated and compared for two different grids.

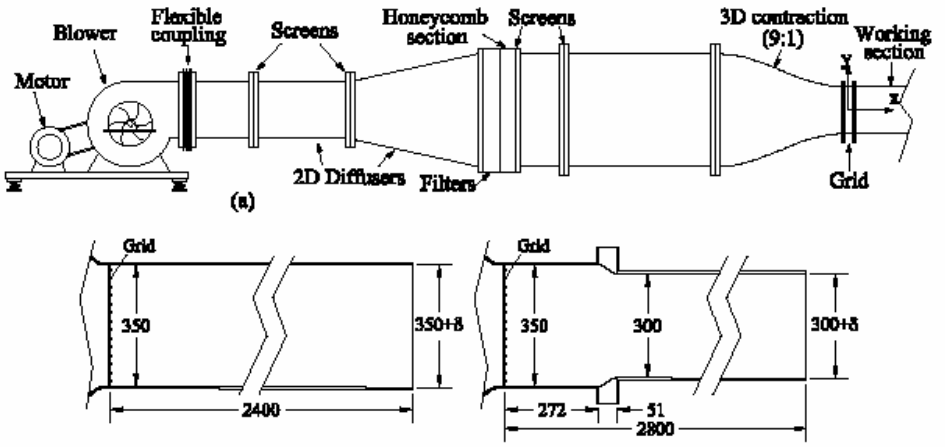

Figure1: Schematic of the wind tunnel (Lavoie *et al.* [10])

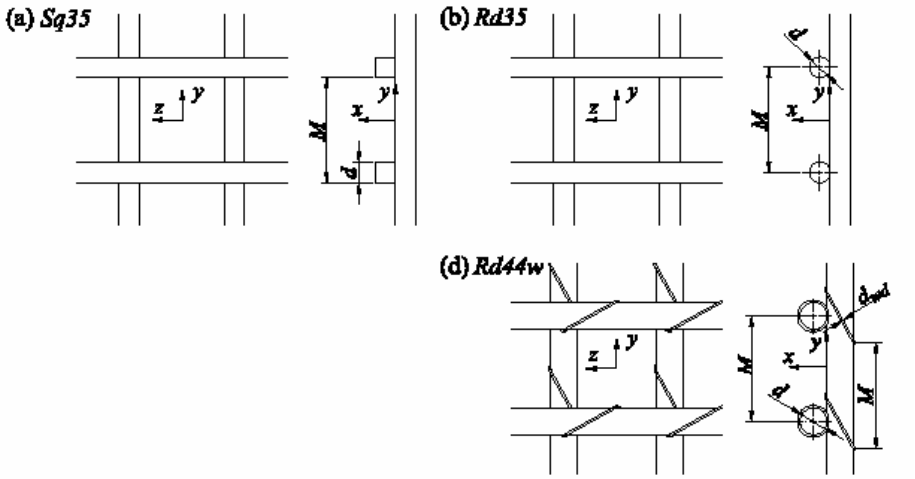

Figure2: Schematic of grid geometries (Lavoie *et al.* [10])

Experimental Conditions

The flow is generated in an open ended wind tunnel with a square section (350mm×350mm, 2.4 m long) as shown in figure 1. The grids are located at the entrance of the working section and their specifications are summarized in table 1. Temperature measurements are carried out at a mean velocity of U = 6.4 m/s on the centreline of the working section downstream of a biplane grid heated mandoline similar to that of Warhaft and Lumley [16] and Sreenivasan *et al.* [14]. The mandoline, of mesh size M_θ=M, is located at a distance of 1.5 M downstream of the grid and is made from a 0.5 mm-diameter chromel-A wire. The heating is implemented as in Zhou *et al.* [17]; the mean temperature increase relative to ambient is sufficiently small (~2 °C) for temperature to be considered passive. The temperature probe consists of one wire operating in a constant current (equal to 0.1 mA) mode. The wire is etched from Wollaston (Pt-10% Rh) to an active length of about 800dw (dw =0.63 μm). The output signals from the constant current circuit are digitized with a 12-bit analog-to-digital converter at a sampling frequency close to 2 f_K (where $f_K = U/2\pi\eta$ is the Kolmogorov frequency) after the low-pass filter cutoff frequency was set to be approximately equal to f_K . Taylor's hypothesis is applied to convert temporal increments to spatial increments. The focus is on how the temperature variance and its dissipation rate decay with the streamwise direction x for the different grid types.

Grid	Geometry	M (mm)	d (mm)	σ	R_M
Sq35	Square	24.76	4.76	0.35	10,564
Rd35	Round	24.76	4.76	0.35	10,564
Rd44w	Round	24.76	6.35	0.44	10,564

Table 1: Geometry of the grids and flow conditions. $\sigma = \frac{d}{M}\left(2 - d/M\right)$ is the grid solidity, and d is the size of the bars. R_M is Reynolds number relative to the mesh size M.

Experimental Results and Scalar Similarity Analysis

Temperature variance decay as for mean turbulent energy can be written as in Zhou *et al*. [17]:

$$\left(\frac{\theta'}{\Delta T}\right)^2 \propto \left(\frac{x}{M} - \frac{x_\theta}{M}\right)^n \qquad (7)$$

where x_θ is the distance between the grid and the mandoline. In our case, this distance was small and did not affect the scaling exponent n. In figure 3, the temperature variance as a function of $(x–x_0)/M$ for x/M between 30 and 100 is plotted. A power law can be fitted to the data over a range extending to a distance of 100M from the grid. For Sq35, Zhou *et al.* [17] found $n = –1.46$ while Antonia *et al.* [3] obtained $n = –1.37$; in the case of the present study, the exponent was –1.11, It would seem that the difference was caused by the secondary contraction. Our exponents compare well with the results of Lavoie *et al.* [10] for the case with contraction.

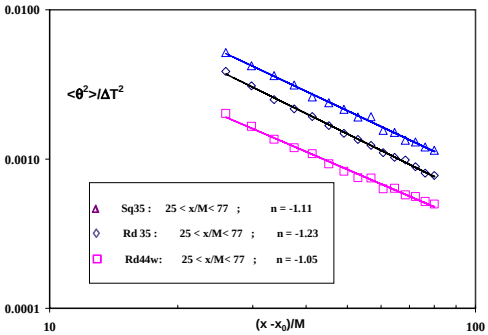

Figure 3: Variation of the normalized temperature variance with x/M for the 3 different grids and $x_0 = x_\theta$. Straight lines are power laws fitted to the data.

For decaying grid turbulence, the transport equations for $\langle\theta^2\rangle$ can be simplified to:

$$\frac{d}{dt}\left(\frac{\langle\theta^2\rangle}{2}\right)+\frac{d}{dx}\left(\frac{\langle\theta^2 u\rangle}{2}\right)+\langle\chi\rangle=0 \qquad (8)$$

$$\langle\chi\rangle = k\left\{\left\langle\left(\frac{\partial\theta}{\partial x}\right)^2\right\rangle+\left\langle\left(\frac{\partial\theta}{\partial y}\right)^2\right\rangle+\left\langle\left(\frac{\partial\theta}{\partial z}\right)^2\right\rangle\right\} \qquad (9)$$

As stated in Zhou *et al.* [17], the second term of the left side equation (8) was about 200 times smaller the other term which leads to:

$$\frac{d}{dt}\left(\frac{\langle\theta^2\rangle}{2}\right)+\langle\chi\rangle=0 \qquad (10)$$

The streamwise decay of $\langle\chi\rangle$ thus followed a power law with a decay exponent of $n–1$. To verify this, $\langle\chi\rangle$ was plotted as a function of $(x–x_0)/M$ for the three grids in figure 4, the same as in figure 3. The agreement between the decay exponents of $\langle\chi\rangle$ and $\langle\theta^2\rangle$ was good and reflected the validity of equation (10) over almost the entire range of measurements.

From figures 3 and 4, one can notice the difference in the decay exponent between the grids which support the finding of Lavoie *et al.* [10] for the decay of mean turbulent energy. In this phase of decay, initial conditions affected the decay law.

If a universal power law exists, its determination is not easy, particularly when it has to be determined over a specific PLDR. Because our data are limited to high values of tU_0/M, a limitation imposed by the experimental setup, we have assumed that Lavoie *et al.*'s [10] determination of the PLDR also applies here. We argue that the similarity of the dynamic field has to be established before that of the scalar field. To correctly determine the power law exponent n, the origin x_0 needs to be determined. With the PLDR, we now have 3 parameters to determine in order to estimate n. In our approach, we combine the method developed by Lavoie et *al.* [10], which is based on fitting to the mean turbulent energy q^2 data, with that of Antonia *et al.* [3] which uses the linearity of λ^2. This linearity is used to infer x_0; as we can see from figure 5 (for grid Sq35), restricting the range to the PLDR yields a smaller value of n with a slightly different x_0.

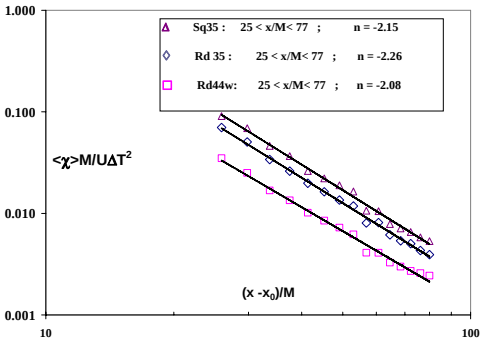

Figure 4: Variation of normalized mean temperature dissipation rate with x/M for the 3 different grids (as in figure 3).

To visualize the effect of restricting the range on the power law exponent, we present in figure 6 (for the same grid) $\langle\theta^2\rangle^{1/n}$ as a function of $(x - x_0)/M$ as in Antonia *et al.* [3], the difference being that, in the present case, x_0 is different from zero (see figure 5).

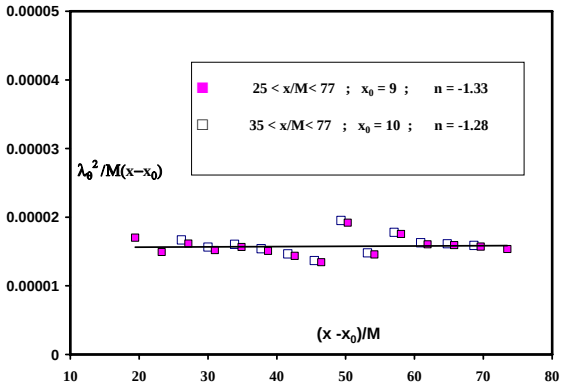

Figure 5: Ratio of λ^2_θ with $(x–x_0)/M$ for different ranges of x/M. Open symbols correspond to the data calculated with $x_0/M = 10$ (with the PLDR from Lavoie [10]; the horizontal line corresponds to $n= –1.28$).

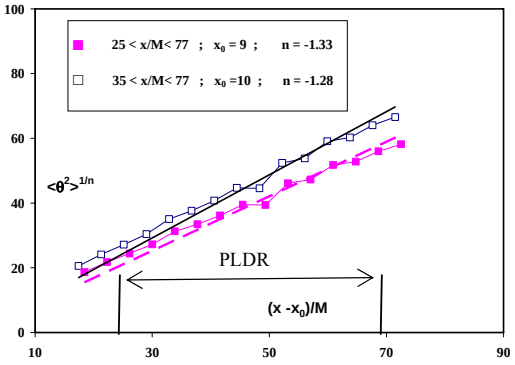

Figure 6: Variation of $\langle\theta^2\rangle^{1/n}$ with $(x–x_0)/M$ obtained from figure 5 (grid Sq35). The straight lines through the origin are least squares regressions to the data.

The two lines represent least-squares regressions to the data and crossing at the origin. In the lower range of x/M, the data are above the line and the opposite for the higher end. The collapse is better in the central region of the PLDR. For the 2 others grids,

this approach is used over the PLDR and x_0 and n are determined, the results are plotted in term of $\langle\chi\rangle^{1/n-1}$ as a function of $(x–x_0)/M$ in figure 7. A good linear variation is observed for the 3 different grids with different slopes as observed earlier. These new exponents are different from the previous ones.

For the 2 others grids, this approach is used over the PLDR and x_0 and I are determined, the results are plotted in terms of $\langle\chi\rangle^{1/n-1}$ as a function of $(x–x_0)/M$ in figure 7. A good linear variation is observed for the 3 different grids with different slopes as observed earlier. These new exponents are different from the previous ones. The Sq35 grid gives an exponent comparable to Antonia *et al.* [3].

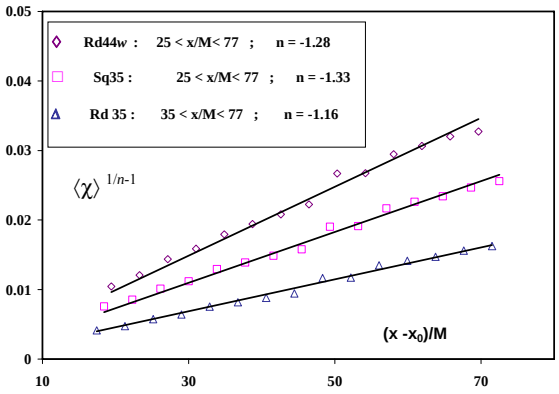

Figure 7: Variations of $\langle\chi\rangle^{1/n-1}$ with $(x–x_0)/M$, x_0 and n are determined as in figure 6. The straight lines through the origin are linear regressions to the data

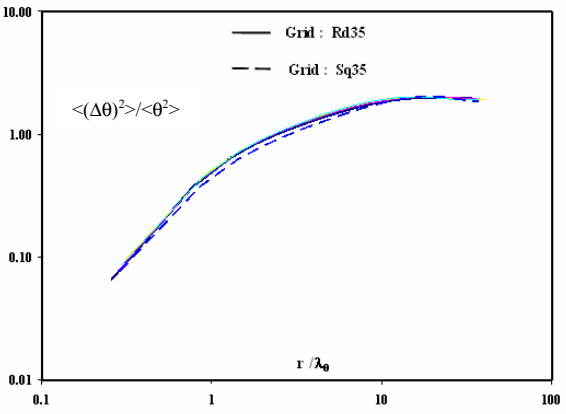

Figure 8: Second-order structure functions of temperature for Rd35 and Sq35.

$$\left\langle \Delta\theta^2 \right\rangle = \left\langle \left[\theta(x+\Delta x)-\theta(x)\right]^2 \right\rangle \qquad (11)$$

Second-order structure functions of temperature (Equation (11)) are represented in figure 8. They are normalized with temperature variances and separation is normalized by Corrsin's length scale λ_θ. The collapse on the solid thick line, which represent the asymptotic state for grid Rd35, is attained at about x/M = 40. For Grid Sq35, the broken line represents the asymptotic curve reached also at about 40 M and it is different from grid Rd35. This is in agreement with Antonia *et al.* [3].

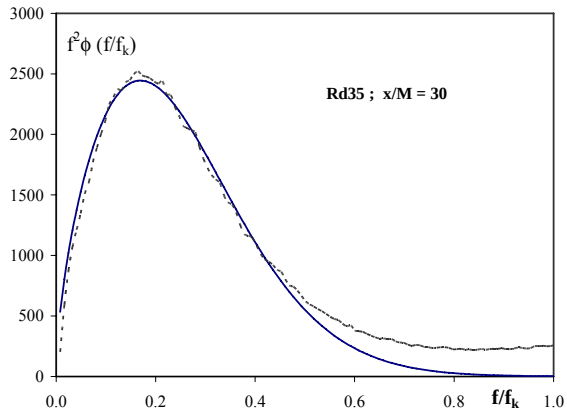

Figure 9: Modelling the dissipation spectrum. The solid line is the model and the broken line is the experimental data for grid rd35 at x/M = 30.

Another approach for studying similarity is to calculate normalized spectra and examine their evolution with x/M. We chose to model the spectra as in Lemay *et al.* [11], viz.

$$\phi\,(f/f_k) \propto f^{-n_\theta} e^{(A(f/f_k)+B(f/f_k)^{1.65}+C)}$$

with A= 1,97, B = –9.33, C = 7.81 and n_θ = 1.42.

The coefficient of proportionality is determined for each position to provide an adequate fit to the experimental data as in Figure 9. Fitting across the inertial and dissipative ranges is also used to calculate the isotropic dissipation rate.

Conclusions

Decaying grid turbulence at low Reynolds numbers ($R_\lambda \sim 50$) depends on initial conditions, irrespectively of whether the mean turbulent energy [5,9,10] or temperature variance is considered. Three different grid geometries are used with heat injected via a mandoline. The power-law exponents for the scalar variance compare are lower than previous results when they were considered over a large range of positions downstream of the grid (30M to 100M**).** This would seem to be caused by the secondary contraction.

The power-law exponent for the isotropic dissipation rate $\langle\chi\rangle$ agrees with that inferred from the temperature variance transport equation, irrespectively of the grid used. Restricting the range of validity of the decay law affects the magnitudes of the effective origin and decay exponent. In this range, the contraction does not seem to affect the behaviour of the scalar as much as that of the turbulent energy. Second-order temperature structure functions collapsed when the temperature variance and the Corrsin microscale λ_θ are used for the normalization. The asymptotic states depend on the initial conditions.

Acknowledgements

The support of Natural Science and Engineering Research Council (NSERC) of Canada is gratefully acknowledged. We are also indebted to P. Lavoie for his contribution.

Nomenclature

A_θ Constant of proportionality
d_w Cold wire diameter
f_k Kolmogorov frequency
k Thermal conductivity
M Mesh size
M_θ Distance between the grid and the Mandoline
n Decay exponent for kinetic energy
n_θ Decay exponent for temperature variance
R_λ Taylor microscale Reynolds number (= $\lambda u'/\nu$)
t Time
x_0 Virtual origin
U Mean velocity
U_0 Free stream velocity approaching the grid
u' Velocity fluctuation (streamwise component)

Symbols

θ Temperature fluctuations
χ Mean temperature dissipation rate
K Wave number
ϕ Power spectrum
η Kolmogorov length scale
σ Solidity ($\sigma = \frac{d}{M}\left(2 - d/M\right)$
λ Taylor microscale ($= u'/(\partial u/\partial x)$)

Subscripts

iso Isotropic
k Kolmogorov

References

[1] Antonia, R.A. & Orlandi, P., Similarity of decaying isotropic turbulence with a passive scalar, *J. Fluid Mech*., **505**, 2004, 123–151.

[2] Antonia, R.A., Ould-Rouis, M., Anselmet, F. & Zhu, Y., Analogy between predictions of Kolmogorov and Yaglom, *J. Fluid Mech.*, **332**, 1997, 395–409.

[3] Antonia, R.A., Smalley, R.J, Zhou, T., Anselmet, F. and Danaila, L., *Physical Review E*, **69**, 2004 016305.

[4] Batchelor, G.K., *The Theory of Homogeneous Turbulence*, Cambridge University Press, 1953.

[5] Burattini, P., Lavoie, P., Agrawal, A., Djenidi, L. & Antonia, R.A., On the Power Law of Decaying Homogeneous Isotropic Turbulence at Low Reynolds Number, Phys. Rev. E, **73**, 2006, 066304.

[6] Comte-Bellot, G. & Corrsin, S. 1966 The Use of a Contraction to Improve the Isotropy of Grid-generated Turbulence, *J. Fluid Mech*., 25, 657–682.

[7] George, W.K., The Decay of Homogeneous Isotropic Turbulence, *Phys. Fluids*, **4**, 1992, 1492–1509.

[8] Lavoie, P., Burattini, P., Djenidi, L. and Antonia, R.A., Effect of Initial Conditions on Decaying Grid Turbulence at Low R_λ, *Exp. Fluids*, **39 (5)**, 2005, 865–874.

[9] Lavoie, P., Djenidi, L. & Antonia, R.A., Effect of Initial Conditions on the Generation of Coherent Structures in Grid Turbulence, in *Whither Turbulence Prediction and Control Conference* (ed. H. Choi) Seoul National University, 2006.

[10] Lavoie, P., Djenidi, L. and Antonia, R.A., Effect of Initial Conditions in Decaying Turbulence Generated by Passive Grids, Under consideration for publication in *J. Fluid Mech*, 2006.

[11] Lemay, J, Benaissa A, Antonia R.A. Correction of Cold-wire Response for Mean Temperature Dissipation Rate Measurements. *Experimental Thermal and Fluid Science*, 27 2003, 133-143

[12] Mohamed, M. S. & LaRue, J. 1990 The decay power law in grid-generated turbulence. *J. Fluid Mech*. 219, 195–214.
Mohamed, M.S. & LaRue, J., The Decay Power Law in Grid-generated Turbulence, *J. Fluid Mech*. **219**, 1990, 195–214.

[13] Speziale, C.G. & Bernard, P.S., The Energy Decay in Self-preserving Isotropic Turbulence Revisited, *J. Fluid Mech*., **241**, 1992, 645–667.Monin, A.S. & Yaglom, A.M., Statistical Fluid Mechanics, vol. 2 . MIT Press, 1975.

[14] Sreenivasan K.R., Tavoularis S., Henry R., Corrsin S. Temperature Fluctuations and Scales in Grid-generated Turbulence. *J. Fluid Mech*, **100**, 1980, 597-291.

[15] Uberoi, M.S., Effect of Wind-tunnel Contraction on Free-stream Turbulence, *J. Aero. Sci*., **23**, 1956, 754–764.

[16] Warhaft, Z. and Lumley, J.L. An Experimental Study of the Decay of Temperature Fluctuations in Grid Generated Turbulence. *J. Fluid Mech*, **88**, 1978, 659-684.

[17] Zhou, T, R.A. Antonia, Chua L.P. Performance of a Probe for Measuring Turbulent Energy and Temperature Dissipation Rates. *Experiment in Fluids,* 33, 2002, 334-345.